Performance Analysis of a Forward Link Channel Estimation Method for Wireless Multicarrier Systems

Xiaofei Dong, *Member, IEEE,* Zhi Ding, *Fellow, IEEE,* and Soura Dasgupta, *Fellow, IEEE*

***Abstract*—We present an effective method for time domain channel estimation of wireless orthogonal frequency division multiplexing (OFDM) system. Relying on a bent-pipe mechanism, the mobile receiver sends a fraction of the received data back to the base station which can then estimate both the forward link and reserve link channel impulse responses. Given knowledge on the forward link channel response, the resource rich base station can employ effective adaptive modulation schemes to increase OFDM system capacity. In this paper, closed-form expressions for channel estimation Cramer Rao lower bound are derived for the feedback system. Impact of feedback parameters on channel estimation performance is discussed through Cramer Rao bound analysis and simulation. Identifiability issues associated with power loaded multicarrier systems are also addressed. Simulation results on the proposed feedback channel estimation scheme are shown.**

***Index Terms*—Adaptive modulation, estimation, feedback communication, frequency division multiplexing, wireless LAN.**

I. Introduction

ORTHOGONAL frequency division multiplexing (OFDM) has been well established as an effective modulation scheme for high speed wireless transmission by utilizing multi-carriers. In practical applications, broadband OFDM wireless systems such as DVB, WiMAX and 3GPP LTE must cope with severe frequency selective distortion on the high data rate forward link (FL) channel. Indeed, forward link channel estimation is needed for both precoding at the transmitter and equalization at the receiver.

Conventional systems achieve OFDM channel identification at the receiver by sending training data on predesignated pilot subcarriers [1], [2], [3]. The channel frequency response on data subcarriers are then estimated from the pilot subcarriers, often via interpolation. As both data rate and discrete Fourier transform (DFT) size grow in high speed multimedia wireless communication systems, complexity of channel estimation becomes a design concern for mobile receivers that often operate on batteries. On the other hand, for wireless systems suffering from severe frequency selective distortions, increasing pilot subcarrier density may be necessary to accurately capture the channel frequency response variation. Transmission of more pilots consumes both power and bandwidth.

To fully exploit the available forward link channel capacity and to achieve good system performance, channel information is desired at the transmitter. It is well known that advanced transmission strategies based on channel state information (CSI), such as adaptive bit and power loading, and subcarrier allocation, are highly effective in improving multicarrier system performance [4]. To implement bit loading, the base-station (BS) transmitter must acquire the information of forward link channels. In conventional approaches, forward link channel knowledge is achieved by letting mobile receivers send back estimated channel parameters through a reliable feedback channel [5]. This process consumes both power and bandwidth of mobile units. Additionally, it also suffers from feedback transmission errors. For these reasons, we generalize the new framework of bent-pipe feedback channel estimation developed for single carrier systems in [6], [7] to multi-carrier systems. In our bent-pipe feedback approach to forward link channel estimation, the mobile device sends back a fraction of the received data to the base station which uses the data to identify the overall round-trip channel (RTC) response. We then apply a subspace algorithm to decouple the forward link (FL) channel response and the reverse link channel (RL) response.

In this work, we present a bent-pipe feedback channel estimation method under adaptive modulation and channel precompensation for OFDM systems. A major contribution of this paper lies in the closed-form Cramer Rao lower bounds (CRLB) analysis for the proposed bent-pipe feedback channel estimates. The CRLB results hold for both single and multi-carrier systems. A detailed analysis on the selection of various design parameters and the impact of the selections on channel estimation performance is also provided. Moreover, we address the issue of channel identifiability when power loading is deployed in the overall systems. We investigate, via numerical simulations, how time variation in mobile channels affects the proposed feedback scheme.

II. OFDM System Model

A conventional single user OFDM transmission and reception system [8] is shown in Fig. 1. Consider the trans-

Manuscript received November 14, 2006; revised June 22, 2007; accepted August 13, 2007. The associate editor coordinating the review of this letter and approving it for publication was C. Xiao. The works published in this paper are supported in part by National Science Foundation Grants, CCF-0515058, CNS-0520126, CCF-0729025, ECS-0622017 and by US Army Research Office Grant W911NF-05-1-0382.

X. Dong is with Altera Corp., San Jose, CA 95134 USA (e-mail: xdong@altera.com).

Z. Ding is with the Department of Electrical and Computer Engineering, University of California, Davis, Davis, CA, 95616 USA (e-mail: zding@ucdavis.edu). He is also currently a guest Changjiang Chair professor of Southeast University, China.

S. Dasgupta is with the Department of Electrical and Computer Engineering, University of Iowa, Iowa City, IA 52446 USA (e-mail: soura-dasgupta@uiowa.edu).

Digital Object Identifier 10.1109/TWC.2008.060939.

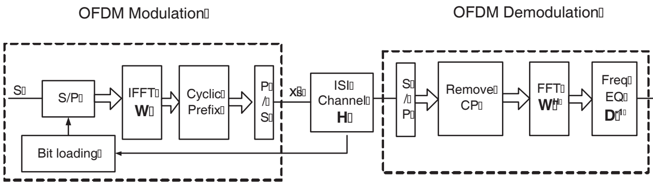

Fig. 1. A DFT-based OFDM system with cyclic-prefix.

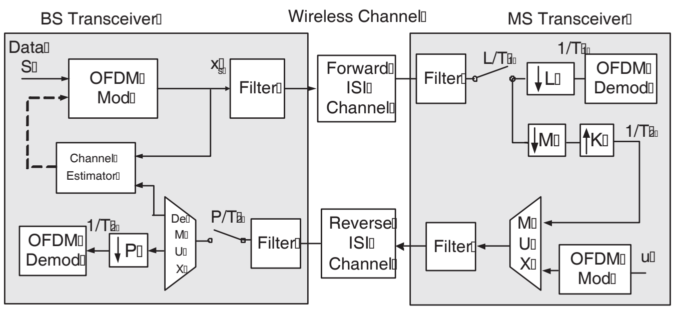

Fig. 2. An OFDM system with decimated feedback.

mission of a single block of information symbols, $\boldsymbol{s} = [s(0)\, s(1) \cdots s(Q-1)]^T$ over Q subcarriers. Denote $\boldsymbol{x}_s$ as the corresponding OFDM symbol where $\boldsymbol{x}_s = \mathbf{W}\boldsymbol{s}$, with $\mathbf{W}$ denoting the $Q \times Q$ IDFT matrix. A cyclic prefix of sufficient length is included in each OFDM symbol $\mathbf{x_s}$ to prevent inter-block interference. At the channel output, after removing the cyclic prefix and DFT, the received signal of the $k-$th orthogonal subchannel is given by

$$r(k) = H_k s(k) + v(k), \quad k = 0, 1, \ldots, Q-1. \tag{1}$$

H_k is the frequency response of subcarrier k, and $v(k)$ is the additive white Gaussian noise. The information data $\boldsymbol{s}$ can be decoded from the received signal of (1) using simple 1-tap frequency scaling.

In the context of wireless communications, our proposed bent pipe feedback OFDM system is shown in Fig. 2. The OFDM modulation and demodulation modules are defined in Fig. 1. Suppose the forward link and the reverse link transmission bandwidth are $1/T_1$ and $1/T_2$, respectively. These transmission data rates are specified by the system. Furthermore, T_1 and T_2 should be chosen such that they can be expressed as $T_1/T_2 = LK/M$ for some integers L, M and K. For example, a popular FL to RL ratio for existing wireless networks is 3:1, which can be realized by choosing $L = 1$, $K = 1$ and $M = 3$. Putting into perspective of our bent-pipe feedback scheme, M and K are the rate changing factors in the mobile station, where M is the downsampling factor and K is the upsampling factor. The mobile station (MS) samples the FL output data at rate L/T_1, and are matched to the RL data rate using a decimator and an interpolator. The converted data can then be multiplexed with the normal reverse link data and sent back to the BS through the RL. We require that integer L and M be coprime, although the decimation and interpolation factor M and K need not be coprime. In fact, they can be equal, which corresponds to the case when forward link and reverse link operate at the same data rate.

When the oversampling ratio is $L = 1$, the forward link

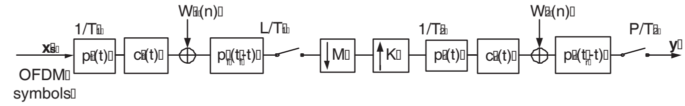

Fig. 3. Signal model of round trip data feedback for channel estimation.

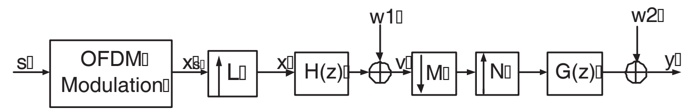

Fig. 4. Discrete signal path of the round trip feedback in OFDM systems.

channel is estimated at baud rate as in [6]. When a larger integer $L > 1$ is chosen, fractionally-spaced FL response can be estimated [7]. To equalize and decode the OFDM data, T-spaced channel information is sufficient. However, fractionally-space sampled algorithm may significantly improve the estimation accuracy at a given data length [7]. The reverse link channel output is oversampled at rate P/T_2, where, similar to the forward link, $P > 1$ gives fractionally-spaced reverse link channel impulse responses.

One key observation is that the mobile can directly sample and retransmit the sampled but otherwise unprocessed OFDM data on the reverse link without additional post-processing or delay. Therefore, the signal path from the base transmitter output, x_s, to the base channel estimator input, y, has a similar structure as the single carrier systems discussed in [7]. An algorithm closely related to [6] [7] can be used in the OFDM system to identify the FL and RL responses.

The feedback signal model of the OFDM system is shown in Fig. 3, where the key difference with a single carrier system is that *the input to the channel*, x_s, is OFDM modulated. $p_f(t)$ and $p_r(t)$ are the responses of the transmitter and receiver filters for the forward link channel and reverse link channel, respectively. $c_f(t)$ and $c_r(t)$ represent the forward link and reverse link multipath channel impulse responses. w_1 and w_2 are the time domain additive white Gaussian noises. u models the normal RL operational data. The feedback data can be combined with the reverse link data via time-multiplexing. Another option is to let the feedback data occupy the reverse link training data slots, since reverse link pilots are no longer needed.

By combining transceiver filters and multipath channels, we denote the overall discrete FL and RL response as $H(z)$ and $G(z)$, respectively. The discrete signal path of the feedback data in the proposed system is shown in Fig. 4, with $N = KP$. Next we present an FL and RL estimation algorithm, and demonstrate its application in OFDM adaptive modulation.

III. FL Channel Estimation Framework

This section provides the basics of our FL channel estimation approach. Although the main approach has been presented earlier in [6], the notations and the precise procedures are reproduced here for OFDM systems in order to analyze and derive the performance (Cramer-Rao) bound.

A. Estimation of RTC

Given access to both its transmitted data and the resulting bent-pipe feedback signal, the base-station can estimate the linear round trip channel. We assume that all signals and noises in Fig. 3 are zero mean, white and mutually uncorrelated, as is the OFDM signal x_s.

Applying type I polyphase decomposition to $H(z)$ and x, we have [9] [10]

$$H(z) = \sum_{i=0}^{M-1} H_i(z^M) z^{-i}, \tag{2}$$

$$x_i(l) = x(lM - i), \quad 0 \le i \le M-1. \tag{3}$$

Type II polyphase decomposition of $G(z)$ and the RTC output y yields

$$G(z) = \sum_{j=0}^{N-1} G_j(z^N) z^{-(N-1-j)}, \tag{4}$$

$$y_j(l) = y(lN + N - 1 - j), \quad 0 \le j \le N-1. \tag{5}$$

Given $x_i(j)$ and $y_j(l)$, we can estimate the (rank one) RTC matrix transfer function [11]

$$\mathbf{F}(z) = \begin{pmatrix} G_0(z) \\ \vdots \\ G_{N-1}(z) \end{pmatrix} \begin{pmatrix} H_0(z) & \cdots & H_{M-1}(z) \end{pmatrix}, \tag{6}$$

where the orders of $G_j(z)$ and $H_i(z)$ are given by

$$l_g = \lceil \frac{l_G + 1}{KP} \rceil - 1 \tag{7}$$

$$l_h = \lceil \frac{l_H + 1}{M} \rceil - 1, \tag{8}$$

in which l_H and l_G are the orders of $H(z)$ and $G(z)$, respectively. $\lceil \cdot \rceil$ denotes ceiling operation. Note that the maximal order of the individual elements of this polynomial matrix is $l_f = l_g + l_h$ for

$$F_{ji}(z) = G_j(z) H_i(z) = \sum_{k=0}^{l_f} f_{ji}(k) z^{-k}. \tag{9}$$

We showed how the round trip channels $F_{ji}(z)$ can be estimated in [11] using the least square approach. Here we only provide the necessary notations to be used later.

Suppose n is the observation window size. Define

$$\boldsymbol{y}_j(k) = (y_j(k) \quad \ldots \quad y_j(k-n+1))^T, \tag{10}$$

$$\boldsymbol{f}_{ji} = (f_{ji}(0) \quad \ldots \quad f_{ji}(l_f))^T, \tag{11}$$

and

$$\mathbf{X}_i(k) = \begin{pmatrix} x_i(k) & \cdots & x_i(k-l_f) \\ \vdots & \vdots & \vdots \\ x_i(k-n+1) & \cdots & x_i(k-l_f-n+1) \end{pmatrix}. \tag{12}$$

Concatenating $\{\mathbf{X}_i(k)\}$ leads to the input data matrix that the BS buffered for channel estimation

$$\mathbf{X}(k) = \begin{pmatrix} \mathbf{X}_0(k) & \mathbf{X}_1(k) & \ldots & \mathbf{X}_{M-1}(k) \end{pmatrix}. \tag{13}$$

The j-th row of the RTC channel matrix to be estimated is the stacked subchannel vectors, given by

$$\boldsymbol{f}_j = (\boldsymbol{f}_{j0}{}^T \quad \ldots \quad \boldsymbol{f}_{j(M-1)}{}^T)^T. \tag{14}$$

Therefore, estimation of the j-th row of $\mathbf{F}(z)$ can be expressed in the time domain as

$$\boldsymbol{y}_j(k) = \mathbf{X}(k)\boldsymbol{f}_j + \boldsymbol{\eta}, \quad 0 \le j \le N-1 \tag{15}$$

where $\boldsymbol{\eta}$ is the noise vector and is uncorrelated with $\mathbf{X}(k)$. As long as $n \ge M(l_f + 1)$, the RTC parameters $\boldsymbol{f}_j$ can be solved in the least square sense,

$$\boldsymbol{f}_j = \mathbf{X}(k)^\dagger \boldsymbol{y}_j, \tag{16}$$

where $(\cdot)^\dagger$ denotes the Moore-Penrose pseudoinverse.

B. Decoupling of FL and RL

Once the RTC response is obtained, a subspace algorithm similar to [12] can be applied to unravel $H(z)$ and $G(z)$ from $\mathbf{F}(z)$ under channel assumptions. The details of the decoupling algorithm is given in Appendix.

C. Identifiability Conditions

As shown in [6], once the RTC response is obtained, to successfully extract FL channel $H(z)$ and RL channel $G(z)$ from RTC $\mathbf{F}(z)$, at least one of the following conditions should be satisfied.

Condition 1: The greatest common divisor (gcd) of the set of polynomials $H_i(z)$ is a pure delay z^{-d} (d integer). In addition, their maximum order is known.

Condition 2: The greatest common divisor (gcd) of the set of polynomials $G_j(z)$ is a pure delay z^{-d} (d integer). Furthermore, their maximum order is known.

With rich scatters either one of the conditions is satisfied with probability one [13].

D. Knowledge Based Multipath Identification

The channel estimation algorithm we just described tries to determine the entire combined channel response which includes the transmitter pulse shaping filter and the receiver matched filter. In most communication systems, however, the only unknown is the multipath channel response. Utilizing the known filter response has been shown to significantly lower the problem complexity [11] [14]. It is simple to show that this knowledge based algorithm [11] is applicable to the OFDM system through fractionally-spaced sampling. The details are given in the Appendix.

E. Discussions

As shown thus far, the proposed bent-pipe scheme enables the OFDM transmitter to identify the FL channel directly. This property is particularly advantageous in OFDM and DMT systems as the channel knowledge can be utilized at the transmitter, for adaptive modulation or power-loading.

In principle, given the FL channel estimate, the base station can take over the 1-tap equalization from the receiver. In this setup, the transmitter is responsible for channel estimation and the simple frequency domain scaling. It can be a useful scheme when the mobile devices are resource-limited.

As shown in (13), the round trip channel is estimated from the input matrix $\mathbf{X}(k)$, which should have full column rank if the input data sequence x_s is persistently exciting [15]. The condition number of the covariance matrix of the OFDM data $\mathbf{X}(k)$ is critical to the accuracy of the least square solution for (15). It is well known [16] that the condition number is upper-bounded by the maximum-to-minimum spectral ratio of the underlying (OFDM) data signal. For single carrier and uniformly modulated OFDM systems, the input data sequence x_s has a white power spectrum density and the covariance matrix is well-conditioned. However, if power loading is used on the frequency domain symbols s to control system capacity, the condition number of the covariance matrix will increase and the accuracy of the least square solution for RTC response may suffer. This is particularly true if some subcarriers are shut down due to power loading. In this case more feedback data may be needed to maintain a good estimate of the round trip channel. Alternatively, we also propose to transmit a low power dummy probing signal on the null subcarriers.

IV. Cramer Rao Lower Bound

In this section we derive the Cramer-Rao lower bound (CRLB) for channel estimates based on the proposed feedback system. The results apply to both single carrier and multicarrier systems. We first consider the CRLB for the T-spaced algorithm. The parameter vector for estimation is the stacked RL and FL channel parameter vectors

$$\boldsymbol{\theta} = \begin{bmatrix} \boldsymbol{g} \\ \boldsymbol{h} \end{bmatrix}, \tag{17}$$

with

$$\boldsymbol{g} = (g_0(0) \ \cdots \ g_0(l_g) \ \cdots \ g_{N-1}(0) \ \cdots \ g_{N-1}(l_g))^T, \tag{18}$$

and

$$\boldsymbol{h} = (h_0(0) \ \cdots \ h_0(l_h) \ \cdots \ h_{M-1}(0) \ \cdots \ h_{M-1}(l_h))^T. \tag{19}$$

$g_j(k)$ and $h_i(k)$ denote the time domain impulse response of channel polyphase components. In the following we first analyze the CRLB for real-valued channel variables.

Let the conditional probability of the bent-pipe feedback data $\mathbf{y}$ given $\boldsymbol{\theta}$ be $f(\mathbf{y}|\boldsymbol{\theta})$. Then the associated Fisher Information Matrix (FIM) can be partitioned into 2×2 blocks, with respect to $\boldsymbol{g}$ and $\boldsymbol{h}$,

$$\mathbf{J} = \begin{bmatrix} \mathbf{J}_{11} & \mathbf{J}_{12} \\ \mathbf{J}_{21} & \mathbf{J}_{22} \end{bmatrix} = E\begin{bmatrix} \frac{\partial \ln f(\boldsymbol{y}|\boldsymbol{\theta})}{\partial \boldsymbol{g}}\left(\frac{\partial \ln f(\boldsymbol{y}|\boldsymbol{\theta})}{\partial \boldsymbol{g}}\right)^H & \frac{\partial \ln f(\boldsymbol{y}|\boldsymbol{\theta})}{\partial \boldsymbol{g}}\left(\frac{\partial \ln f(\boldsymbol{y}|\boldsymbol{\theta})}{\partial \boldsymbol{h}}\right)^H \\ \frac{\partial \ln f(\boldsymbol{y}|\boldsymbol{\theta})}{\partial \boldsymbol{h}}\left(\frac{\partial \ln f(\boldsymbol{y}|\boldsymbol{\theta})}{\partial \boldsymbol{g}}\right)^H & \frac{\partial \ln f(\boldsymbol{y}|\boldsymbol{\theta})}{\partial \boldsymbol{h}}\left(\frac{\partial \ln f(\boldsymbol{y}|\boldsymbol{\theta})}{\partial \boldsymbol{h}}\right)^H \end{bmatrix}. \tag{20}$$

Applying the block matrix inversion formula [17], the CRLB for FL channel estimation is given by

$$CRB_h = (\mathbf{J}_{22} - \mathbf{J}_{21}(\mathbf{J}_{11})^{-1}\mathbf{J}_{12})^{-1}. \tag{21}$$

Similarly, CRLB for RL channel estimation is given by

$$CRB_g = (\mathbf{J}_{11} - \mathbf{J}_{12}(\mathbf{J}_{22})^{-1}\mathbf{J}_{21})^{-1}. \tag{22}$$

A. Conditional Probability Density Function

To simplify the notation, we start with the case when $N = 1$, i.e. no interpolation nor upsampling. We later extend the results to the more complicated cases when $N \neq 1$ and when the forward link channel is oversampled.

Let the forward link polyphase components be coprime. Our goal is to estimate FL and RL channel responses from

$$y(z) = G(z)\begin{bmatrix} H_0(z) & \cdots & H_{M-1}(z)\end{bmatrix}\begin{bmatrix} x_0(z) \\ \vdots \\ x_{M-1}(z)\end{bmatrix} + G(z)W_{10}(z) + W_2(z). \tag{23}$$

$W_{10}(z)$ and $W_2(z)$ denote the noise polyphase.

We now introduce a notation for polynomial matrix convolution. For a polynomial $A(z)$ of the maximal order l, define the $m \times (l+m)$ Toeplitz filtering matrix as

$$\mathcal{T}_m(A) = \begin{pmatrix} A(0) & \cdots & A(l) & & \\ & \ddots & \ddots & \ddots & \\ & & A(0) & \cdots & A(l) \end{pmatrix}. \tag{24}$$

Taking signal samples of (23) from time instant t_0 with observation window size n, the signal portion is

$$\begin{bmatrix} y(t_0) & \cdots & y(t_0-n+1)\end{bmatrix}^T = \mathcal{T}_n(G)\sum_{i=0}^{M-1}\mathcal{T}_{n+l_g}(H_i)\begin{bmatrix} x_i(t_0) \\ \vdots \\ x_i(t_0-n-l_f+1)\end{bmatrix}. \tag{25}$$

Using the notation in (12) but taking only the first l_g+1 columns of each submatrix $\mathbf{X}_i(t_0-k)$, we define

$$\mathbf{X}(t_0-k) = \begin{bmatrix}\mathbf{X}_0^T(t_0-k) & \cdots & \mathbf{X}_{M-1}^T(t_0-k)\end{bmatrix}^T, \tag{26}$$

where $\mathbf{X}(t_0-k)$ has dimension $M(l_h+1)\times(l_g+1)$. Therefore (25) can be rewritten in a compact form as

$$\boldsymbol{y}(t_0) \stackrel{\text{def}}{=} \begin{bmatrix} y(t_0) & \cdots & y(t_0-n+1)\end{bmatrix}^T = (\mathbf{I}_n \bigotimes \boldsymbol{h}^T)\underbrace{\begin{bmatrix}\mathbf{X}^T(t_0) & \cdots & \mathbf{X}^T(t_0-n+1)\end{bmatrix}^T}_{\stackrel{\text{def}}{=}\mathbf{Z}_\mathbf{X}}\boldsymbol{g}, \tag{27}$$

where $\bigotimes$ denotes vector product, and $\mathbf{Z}_\mathbf{X}$ is a matrix of dimension $nM(l_h+1)\times(1+l_g)$.

Similarly, we can express each received sample $y(t_0-k)$ as a function of the FL channel vector $\boldsymbol{h}$, given by

$$y(t_0-k) = \begin{bmatrix}\vec{x}_0(t_0-k) & \cdots & \vec{x}_{M-1}(t_0-k)\end{bmatrix} (\mathbf{I}_{M(l_h+1)}\bigotimes \boldsymbol{g})\boldsymbol{h}, \tag{28}$$

where $\vec{x}_i(t_0-k)$ is a $1\times(l+l_g)(1+l_h)$ row vector, constructed using the data from the i-th polyphase component of the FL data x,

$$\vec{x}_i(t_0-k) = \begin{bmatrix}\boldsymbol{x}_i(t_0-k) & \cdots & \boldsymbol{x}_i(t_0-k-l_h)\end{bmatrix} \tag{29}$$

with

$$\boldsymbol{x}_i(t_0-k-j) = \begin{bmatrix} x_i(t_0-k-j) & \cdots & x_i(t_0-k-j-l_g)\end{bmatrix}. \tag{30}$$

Consequently, (25) can also be written as

$$\boldsymbol{y}(t_0) = \underbrace{\begin{bmatrix} \vec{x}_0(t_0) & \cdots & \vec{x}_{M-1}(t_0) \\ \vec{x}_0(t_0-1) & \cdots & \vec{x}_{M-1}(t_0-1) \\ \vdots & \cdots & \vdots \\ \vec{x}_0(t_0-n+1) & \cdots & \vec{x}_{M-1}(t_0-n+1) \end{bmatrix}}_{\stackrel{\text{def}}{=}\mathbf{S_X}} \times (\mathbf{I}_{M(l_h+1)} \bigotimes \boldsymbol{g})\boldsymbol{h}. \quad (31)$$

$\mathbf{S_X}$ has dimension $n \times M(1+l_h)(1+l_g)$. Define

$$\mathbf{Z} = (\mathbf{I}_n \bigotimes \boldsymbol{h})\mathbf{Z_X}, \quad (32)$$

$$\mathbf{S} = \mathbf{S_X}(\mathbf{I}_{M(l_h+1)} \bigotimes \boldsymbol{g}). \quad (33)$$

We can express the system equation (23) as

$$\boldsymbol{y}(t_0) = \mathbf{Z}\boldsymbol{g} + \boldsymbol{\eta} = \mathbf{S}\boldsymbol{h} + \boldsymbol{\eta}, \quad (34)$$

where $\boldsymbol{\eta}$ denotes the colored noise. The correlation matrix $\boldsymbol{\Omega}$ of $\boldsymbol{\eta}$ is given by

$$\boldsymbol{\Omega} = \sigma_{w_1}^2 \mathcal{T}_m(G)\mathcal{T}_m^H(G) + \sigma_{w_2}^2. \quad (35)$$

Given a set of channels and signals as parameter vector θ, $\boldsymbol{y}(t_0)$ is Gaussian with probability density function

$$f(\boldsymbol{y}|\boldsymbol{\theta}) = \frac{1}{(2\pi)^{\frac{n}{2}}|\boldsymbol{\Omega}|^{\frac{1}{2}}} \exp\{-\frac{1}{2}(\boldsymbol{y}-\mathbf{S}\boldsymbol{h})^H\boldsymbol{\Omega}^{-1}(\boldsymbol{y}-\mathbf{S}\boldsymbol{h})\}. \quad (36)$$

B. Partial Derivatives of the Likelihood Function

Note that both the signal and the noise of (36) are functions of the reverse link channel response. Taking derivative of the logarithm of (36) with respect to the vector $\boldsymbol{g}$, we have

$$\frac{\partial \ln f(\boldsymbol{y}|\boldsymbol{\theta})}{\partial \boldsymbol{g}} = -\frac{1}{2}\frac{\partial \ln \det(\Omega)}{\partial \boldsymbol{g}} + \mathbf{Z}^H\boldsymbol{\Omega}^{-1}\boldsymbol{\eta} - \frac{1}{2}\frac{\partial \boldsymbol{\eta}^H\boldsymbol{\Omega}^{-1}\boldsymbol{\eta}}{\partial \boldsymbol{g}}. \quad (37)$$

Using established matrix calculus results, we have

$$u_i = \frac{1}{2}\frac{d}{dg_i}\{\boldsymbol{\eta}^H\boldsymbol{\Omega}^{-1}\boldsymbol{\eta}\} = -\sigma_{w_1}^2 \mathrm{Tr}\{\boldsymbol{\Omega}^{-1}\boldsymbol{\eta}\boldsymbol{\eta}^H\boldsymbol{\Omega}^{-1}[\mathcal{T}_n^H(\boldsymbol{g})]_i\}; \quad (38)$$

$$v_i = \frac{1}{2}\frac{d}{dg_i}\ln\det\{\boldsymbol{\eta}^H\boldsymbol{\Omega}^{-1}\boldsymbol{\eta}\} = \sigma_{w_1}^2 \mathrm{Tr}\{\boldsymbol{\Omega}^{-1}[\mathcal{T}_n^H(\boldsymbol{g})]_i\} \quad (39)$$

where $[\mathbf{A}]_i$ denotes the $n \times n$ sub-matrix of an $(n+l_g) \times m$ $\mathbf{A}$ from the i-th row to $(i+n-1)$-th row. Stacking the derivatives into a vector, we have $\boldsymbol{v} = \begin{bmatrix} v_1 & \cdots & v_{l_g+1} \end{bmatrix}$, and $\boldsymbol{u} = \begin{bmatrix} u_1 & \cdots & u_{l_g+1} \end{bmatrix}$. It is easy to see that $E\{\boldsymbol{u}\} = \boldsymbol{v}$.

C. CRLB for FL Estimation

Using the results from (38) and (39) as well as the equality of (34), the CRLB for channel estimation can be calculated. We re-write (37) as

$$\frac{\partial \ln f(\boldsymbol{y}|\boldsymbol{\theta})}{\partial \boldsymbol{g}} = -\boldsymbol{v} + \mathbf{Z}^H\boldsymbol{\Omega}^{-1}\boldsymbol{\eta} + \boldsymbol{u}. \quad (40)$$

Substituting it into the definition of FIM, we have

$$\mathbf{J}_{11} = \mathbf{Z}^H\boldsymbol{\Omega}^{-1}\mathbf{Z} + 3\boldsymbol{v}\boldsymbol{v}^H + \mathrm{E}\{\boldsymbol{u}\boldsymbol{u}^H\}. \quad (41)$$

Define a matrix $\mathbf{T} = \mathrm{E}\{\boldsymbol{u}\boldsymbol{u}^H\}$. Obviously its (i,j)-th element $\mathbf{T}_{ij}$ involves the fourth-order statistics of a multivariate Gaussian vector $\boldsymbol{\eta}$ that can be evaluated from their second order statistics. We note, however, that neither $\boldsymbol{v}$ nor $\mathbf{T}$ is a function of the feedback data. As a result, with sufficient SNR, the impact of these two terms is negligible. We can therefore approximate the FIM at high SNR using

$$\mathbf{J}_{11} = \mathbf{Z}^H\boldsymbol{\Omega}^{-1}\mathbf{Z}. \quad (42)$$

Combining (34) and (37), the other FIM blocks are

$$\mathbf{J}_{12} = \mathbf{Z}^H\boldsymbol{\Omega}^{-1}\mathbf{S} = \mathbf{J}_{21}^H, \quad (43)$$

$$\mathbf{J}_{22} = \mathbf{S}^H\boldsymbol{\Omega}^{-1}\mathbf{S}. \quad (44)$$

Given the expressions of the FIM, the CRLB for both the FL and the RL channels can be obtained.

As expected, when we let the noise variance be a known quantity instead of a parameter to estimate, the $(2+l_g+l_h) \times (2+l_g+l_h)$ Fisher Information Matrix of $\boldsymbol{\theta}$ is rank deficient, and its rank is $1+l_g+l_h$. In particular, $\boldsymbol{h}$ is a right singular vector. This implies that the feedback channel estimation has an intrinsic scalar ambiguity [18] [19]. This is consistent with our observation that without additional information, any decoupling algorithm can only separate $G(z)$ and $H(z)$ up to a scalar. Consequently, $\mathbf{J}_h \stackrel{\text{def}}{=} \mathbf{J}_{22} - \mathbf{J}_{21}(\mathbf{J}_{11})^{-1}\mathbf{J}_{12}$ is also rank deficient, and the CRLB for forward link channel in (21) technically equals infinity. To arrive at a meaningful CRLB, special care must be taken.

As shown in [18], the pseudo-inverse of $\mathbf{J}_h$ can be interpreted as the CRLB if the projection of $\boldsymbol{h}$ along the null space of $\mathbf{J}_h$ is known. This is equivalent to knowing explicitly the scalar ambiguity. Therefore, we use the Moore-Penrose pseudo-inverse instead of inverse of $\mathbf{J}_h$ for calculating CRLB for the forward link channel:

$$CRLB_h \geq (\mathbf{J}_{22} - \mathbf{J}_{21}(\mathbf{J}_{11})^{-1}\mathbf{J}_{12})^{\dagger}. \quad (45)$$

Similarly, the CRLB for the reverse link channel estimation is obtained by taking pseudo-inverse of (22):

$$CRLB_g \geq (\mathbf{J}_{11} - \mathbf{J}_{12}(\mathbf{J}_{22})^{-1}\mathbf{J}_{21})^{\dagger}. \quad (46)$$

Note that the CRLB in (42), (43) and (44) are for real-valued channel parameters. For complex parameters, we can follow the notation used in [18] and obtain similar results. The derivation details are tedious and are omitted here.

D. CRLB for Alternative Parameterizations

When the forward link channel is oversampled at the mobile receiver, the feedback signal $x(n)$ used to construct (27), (31), (32) and (33) is the base station data interpolated by a factor L. The derivation of CRLB for both FL and RL channels remains the same. Note, however, that the true unknowns in the forward link channel estimation are merely the multipath coefficients. Thus, we may replace $\boldsymbol{h}$ by $\mathcal{T}_{l_{c_f}}^T(P_f)\boldsymbol{c}_f$, where $\boldsymbol{c}_f$ is the vector being estimated.

If the mobile station has an N-fold interpolator after the decimator, the reverse link channel parameter we need to estimate becomes $\boldsymbol{g} = \begin{bmatrix} \boldsymbol{g}_0^T & \boldsymbol{g}_1^T & \cdots & \boldsymbol{g}_{N-1}^T \end{bmatrix}^T$. Stacking the polyphase components of the round trip channel output, (27) becomes

$$\begin{bmatrix} \boldsymbol{y}_0(t_0) \\ \vdots \\ \boldsymbol{y}_{N-1}(t_0) \end{bmatrix} = \underbrace{\begin{bmatrix} (\mathbf{I}_n \otimes \boldsymbol{h})\mathbf{Z}_\mathbf{X} \\ \vdots \\ (\mathbf{I}_n \otimes \boldsymbol{h})\mathbf{Z}_\mathbf{X} \end{bmatrix}}_{\mathbf{Z}} \boldsymbol{g}. \tag{47}$$

Similarly, the input-output equation using $\boldsymbol{h}$ as the unknown changes to

$$\begin{bmatrix} \boldsymbol{y}_0(t_0) \\ \vdots \\ \boldsymbol{y}_{N-1}(t_0) \end{bmatrix} = \underbrace{\begin{bmatrix} \mathbf{S}_\mathbf{X}(\mathbf{I}_{M(l_h+1)} \otimes \boldsymbol{g}_0) \\ \vdots \\ \mathbf{S}_\mathbf{X}(\mathbf{I}_{M(l_h+1)} \otimes \boldsymbol{g}_{N-1}) \end{bmatrix}}_{\mathbf{S}} \boldsymbol{h}. \tag{48}$$

The new noise correlation is

$$\begin{aligned} \mathcal{Q} = \mathrm{E}\{\boldsymbol{\eta}\boldsymbol{\eta}^H\} &= \mathrm{E}\left\{ \begin{bmatrix} \boldsymbol{\eta}_0 \\ \vdots \\ \boldsymbol{\eta}_{N-1} \end{bmatrix} \begin{bmatrix} \boldsymbol{\eta}_0 & \cdots & \boldsymbol{\eta}_{N-1} \end{bmatrix}^H \right\} \\ &= diag((\boldsymbol{\Omega}_0 \quad \boldsymbol{\Omega}_1 \quad \boldsymbol{\Omega}_{N-1}) \end{aligned} \tag{49}$$

where $\boldsymbol{\Omega}_i$ is defined in (35). Given these quantities, the exact expression for the FIM with forward link channel oversampling can be derived. At high SNR, we can use the simplified approximation (42) by replacing $\boldsymbol{\Omega}$ with $\mathcal{Q}$.

E. Impact of Feedback Design Parameters

In practical systems the choice of decimation factor M and interpolation factor K depends on the desired ratio of the forward link and reverse link data rate. They are reconfigurable parameters.

Generally speaking, a large decimation factor M reduces the estimation accuracy of the round trip channel $\mathbf{F}(z)$ and consequently the estimation accuracy for both the forward link and reverse link channels. Intuitively, a larger M means that more round trip channel coefficients must be estimated from the same number of observed data. This can be seen from the asymptotic CRLB for the round trip channel estimation, where for i.i.d. noise, the CRLB reduces to

$$CRLB_f \xrightarrow{p.} \frac{\sigma_\eta^2}{n\sigma_x^2}\mathbf{I}_{(l_f+1)M}. \tag{50}$$

Therefore, the trace of the CRLB for the round trip estimation scales with M,

$$\mathrm{Tr}\{CRLB_f\} = \frac{\sigma_\eta^2 M(l_f+1)}{n\sigma_x^2} = \frac{\sigma_\eta^2(Ml_g+l_H)}{n\sigma_x^2}. \tag{51}$$

(51) can approximate the impact of M on the performance when the sample size is large. For other cases, the CRLB for $\boldsymbol{h}$ and $\boldsymbol{g}$ can be obtained precisely for every specified value of M, as shown previously.

It is also worth mentioning that large decimation factor M requires the BS to buffer more forward link data for channel estimation, as the buffer size N_{buffer} is given by

$$N_{\text{buffer}} = (n+l_h)M \tag{52}$$

where n is the number of feedback data on the RL.

In practical systems, an important benefit of choosing a large decimation factor M is that it makes the coprimeness condition easier to satisfy, thereby improving the robustness of the feedback channel estimation algorithm. If the FIR channel is long, near-zero polyphase components in the channel could make the channel matrix $\mathcal{T}_n(\mathbf{H})$ nearly singular. Consequently, the subspace channel decoupling algorithm may fail. By distributing the channel information over a larger dimension through polyphase decomposition, the order of the polyphase component along each dimension is reduced, and the chance of having coprime subchannels is greatly increased.

In terms of the interpolation factor K, we note that large K factor compromises channel estimation accuracy. On one hand, for $K > 1$, zeros are inserted in the feedback sequence. These zeros do not carry FL channel information, and the relative number of input data available to solve the round trip channel response is reduced. On the other hand, K reduces the average feedback data SNR, which is given by

$$SNR_j = \frac{\mathrm{E}\{\|\boldsymbol{y}_j\|^2\}}{\mathrm{E}\{\|\boldsymbol{\eta}_j\|^2\}} = \frac{\sigma_{x_s}^2\|\boldsymbol{g}_j\|^2\|\boldsymbol{h}\|^2}{\sigma_{w_1}^2\|\boldsymbol{g}_j\|^2 + \sigma_{w_2}^2} \tag{53}$$

for $j = 0, \cdots, K-1$. $\|\cdot\|$ denotes the norm. Let x_s be the time domain OFDM symbol for transmission. If each subchannel $\boldsymbol{g}_j$ has approximately $1/K$ of the total power of $\|\boldsymbol{g}\|^2$, then (53) can be reduced to

$$SNR_j = \frac{\sigma_{x_s}^2}{\sigma_w^2(1+K)}, \tag{54}$$

when channel responses are normalized to unit power. To get the exact CRLB for the forward link and reverse link channel estimation, results from the previous section can be used.

V. Numerical and Simulation Results

We consider a 256-carrier OFDM system using quadrature amplitude modulation (QAM). The channel bandwidth is 2.5MHz, with cyclic prefix size $1/16$ of the DFT size. Let the OFDM frame duration be 1 *ms*. The channel is a two-ray multipath channel [20]

$$c(t) = \alpha_1\delta(t) + \alpha_2\delta(t-\tau). \tag{55}$$

Matching root-raised cosine filters are used at the transmitter and receiver with pulses truncated to 3 symbol periods. We should not confuse the fractionally spaced two-ray multipath channel with channel delay spread, which must include both transmitter and receiver pulse shaping filters and is much longer than two symbol periods.

The signal to noise ratio (SNR) is defined as the average sampled data SNR at the channel output, i.e., for the FL, the SNR is given by

$$\mathrm{SNR_f} = \frac{\sigma_{x_s}^2}{\sigma_{w_1}^2}\frac{\sum\|h(k)\|^2}{\sum\|p_f(k)\|^2}, \tag{56}$$

where $h(k)$ and $p_f(k)$ are T-spaced samples of the channel and the filter. Similarly, the reverse link signal power is defined according to the normal message data, u, which gives

$$\mathrm{SNR_r} = \frac{\sigma_u^2}{\sigma_{w_2}^2}\frac{\sum\|g(k)\|^2}{\sum\|p_r(k)\|^2}. \tag{57}$$

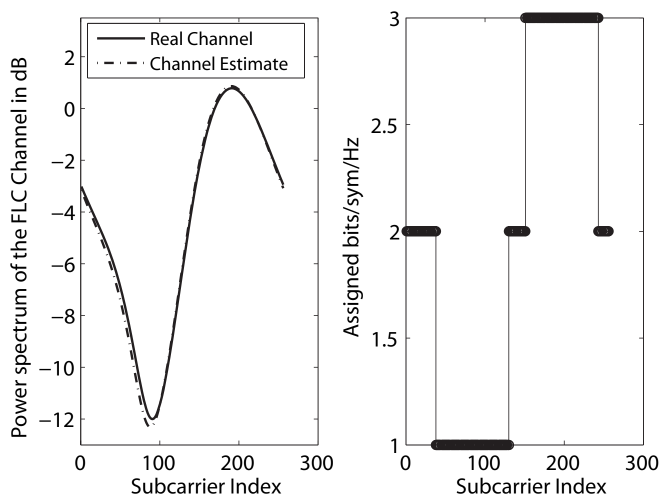

Fig. 5. Multipath channel frequency response and bit loading result using [4].

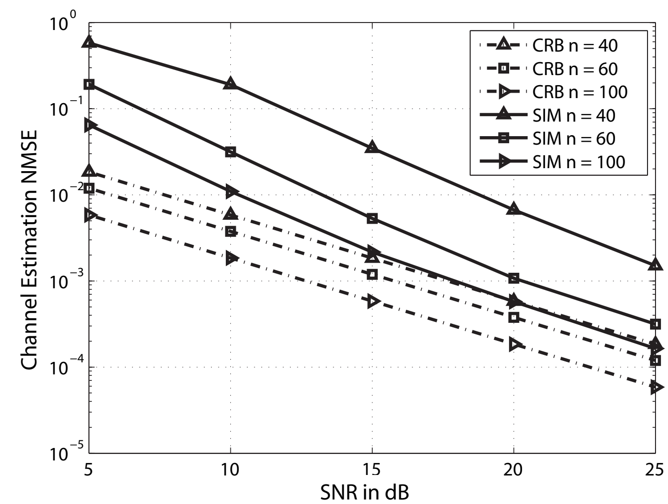

Fig. 6. Forward link channel estimation Cramer Rao lower bound v.s. simulated NMSE.

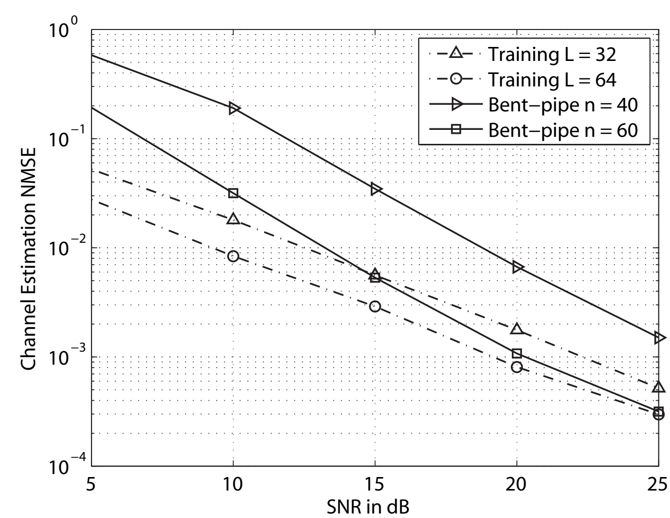

Fig. 7. Comparison of the training based method and the bent-pipe feedback method.

The channel is estimated at the same average SNR as the data decoding. Note that the SNR is defined on the receiving data SNR. Therefore the effective SNR on the feedback data received in the base station is less than the data $\mathrm{SNR_r}$ and $\mathrm{SNR_f}$. This is because of its inclusion of not only the RL noise, but also FL noise. As we will demonstrate in the following simulation results, the proposed channel estimation method performs well even with the reduced effective SNR.

In simulations, we assume $\sigma_{w_1}^2 = \sigma_{w_2}^2 = \sigma_w^2$. We also let the FL data x_s and the RL data data u have the same variance, i.e. $\sigma_{x_s}^2 = \sigma_u^2$, and let the data SNR on the FL and RL be equal, $\mathrm{SNR_f} = \mathrm{SNR_r}$. The performance of channel estimation is measured by the normalized mean square error (NMSE):

$$NMSE = \frac{1}{\|\mathbf{h}\|^2}\left(\frac{1}{M_t}\sum_{i=1}^{M_t}\|\hat{\mathbf{h}}_i - \mathbf{h}\|^2\right), \qquad (58)$$

where M_t is the number of Monte Carlo runs, $\hat{\mathbf{h}}_i$ is the estimation from the i-th trial, and $\mathbf{h}$ is the true channel. In calculations, NMSE results are averaged over 100 Monte Carlos trials.

Since feedback data only consumes reverse link bandwidth and there is no forward link training, we use the number of feedback data on the RL as a design parameter. The bit-loading and power allocation method we used in the simulation was first introduced by Chow and Cioffi in [4]. This finite granularity loading algorithm approximates the water pouring distribution iteratively on a subcarrier by subcarrier basis. Fig. 5 shows a typical channel frequency response used in the simulation and its bit loading results.

A. Performance of Channel Estimation Algorithm

Fig. 6 compares the CRLB and the simulation results of the channel estimation NMSE. Uniformly modulated QPSK data are sent to the mobile station on the forward link. The complex Gaussian multipath channels are randomly picked such that the FL multipath channel has $\alpha_1 = -0.1581 + 0.2841i$, $\alpha_2 = -0.1303 - 1.2193i$ with $\tau = T/2$, while the RL channel has $\alpha_1 = 0.3022 + 0.5827i$, $\alpha_2 = 0.6987 - 0.4264i$ with $\tau = T/3$. Decimation by $M = 3$ is used, and FL channel output is oversampled by a factor of $L = 2$. No interpolation is used and reverse link channel output is baud rate sampled. The dashed lines show the numerical CRLB value (45). Clearly, as we increase the number of reverse link feedback data n, the channel estimation accuracy improves. The gap between simulation results and the performance lower bound also reduces with more feedback data.

We also compare the channel estimation with the conventional training based method. Assume BPSK modulated forward link pilots are used on equally spaced pilot subcarriers for a 256-OFDM system. Assume the pilot locations and ISI channel length are known. A maximum-likelihood (ML) estimator or least square (LS) estimator [1] can be used to obtain the time domain channel impulse response estimate. In Fig. 7, we compare channel estimation error of the bent-pipe algorithm with conventional frequency domain training through simulation. L is the number of pilot subcarriers, and n is the number of feedback data on the reverse link channel for the bent-pipe feedback algorithm. The same channel response is used as in Fig. 6. The training method uses a pilot subcarrier spacing of 8 and 4 respectively, corresponding to 32 and 64 forward link pilot subcarriers.

Fig. 7 clearly demonstrates an advantage of the bent-pipe feedback algorithm in terms of total transmission bandwidth saving. With the same transmission power, both methods have comparable channel estimation performance. Even although the training algorithm in general has slightly smaller channel estimation errors, particularly at low SNR, the training process requires considerably more total bandwidth. In addition to the forward link pilot symbols, the training based algorithm also requires reverse link training to estimate the RL channel. If forward link CSI feedback is required, additional RL bandwidth is necessary. As shown in Fig. 7, with similar bandwidth overhead, the training method only identifies the FL channel at the mobile station, while the bent-pipe algorithm allows the base station to identify both FL and RL channels. Also, the bandwidth overhead for bent-pipe feedback occurs only on the reverse link, thus preserving the often more precious forward link bandwidth for information transmission.

B. Quasi-Static Channels

We now consider the bit and symbol error performance of an OFDM system in quasi-static channels. The feedback channel estimation is activated without adaptive modulation or precompensation modules in the system as the channel is assumed to be unknown. Once the FL channel is estimated, it is used to design bit and power loading or 1-tap frequency transmitter pre-scaling, as described earlier. Fig. 8 compares the forward link bit error rate (BER) of OFDM systems with and without adaptive modulation. The BER results are tested over 100 random complex Gaussian channels. The channels are estimated at the same SNR as receiver decoding. The knowledge based algorithm is used to lower feedback length and it uses $n = 45$ reverse link feedback data.

For comparison, the results of bit-loading and receiver detection under perfect channel knowledge are also presented. As expected, the adaptive modulation significantly improves the error rate performance, particularly at high SNR. This is due to the fact that when the OFDM subcarriers are uniformly modulated, the errors are dominated by subchannels in deep fades. Boosting signal power only has very limited effect.

The bit loaded OFDM performance for target data rate $3\ b/sym/Hz$ is at least $5\ dB$ worse than the low rate system at $2\ b/sym/Hz$, and the gap grows as SNR increases. This is consistent with the observation in [21]. With bit loading, higher total data rate requires high SNR subcarriers to carry even more bits, thus becoming more vulnerable to noise and interference.

It is worth mentioning that correct knowledge of the ISI channel length is critical to converting our time domain channel estimate to frequency domain subcarrier gains. When the ISI channel has small leading or trailing taps, these small taps are hard to estimate accurately. However, errors in these parameters may still lead to large errors in the frequency domain. Without knowing the exact channel order, using under-estimated channel length often provides a more accurate channel frequency response than using over-estimated channel order.

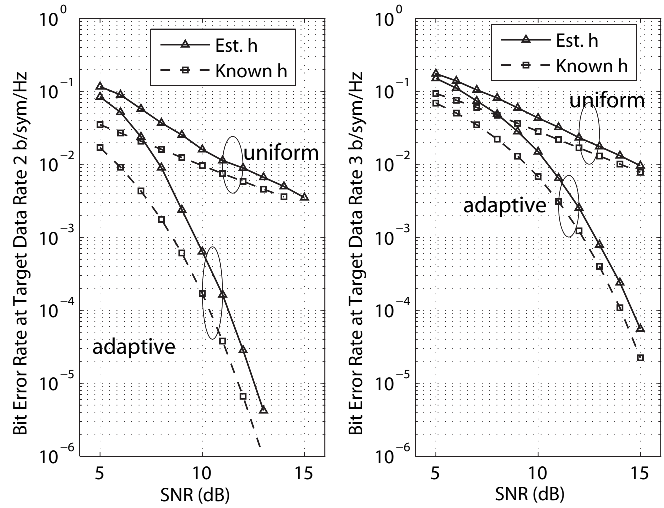

Fig. 8. Bit error rate comparison of a bit loaded and uniformly modulated static OFDM system with different target data rates.

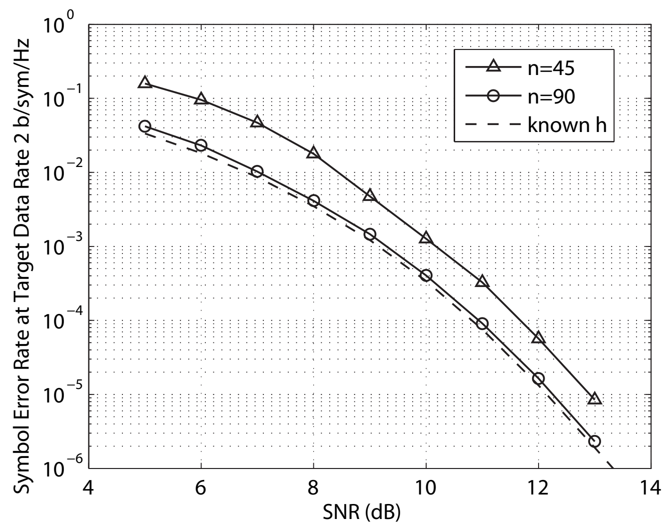

Fig. 9. Symbol error rate comparison of a bit loaded static OFDM system using different feedback data length.

C. Impact of Imperfect Channel Knowledge

Channel estimation errors affect OFDM systems at two places: the bit loading module and the decoding module. As manifested in Fig. 8, for both the bit loaded and the uniform OFDM modulations, the error rate curves converge to the results obtained from perfect channel knowledge.

Our simulation results showed that by using 45 RTC feedback symbols, the NMSE of channel estimation is reduced to under 10^{-3} with a mild SNR of 10-13dB. The performance loss of the system using our channel estimate is kept under $1\ dB$ of the perfect channel case. This confirms the analytical results for bit error rate as a function of NMSE for OFDM systems in [21].

There is a tradeoff between FL channel estimation accuracy and RL bandwidth consumption. This is reflected in Fig. 9 which compares the symbol error rate of a bit loaded OFDM system utilizing channel estimates of various degrees of accuracy. The performance degradation due to estimation NMSE is evident at low SNR. However, by increasing the feedback

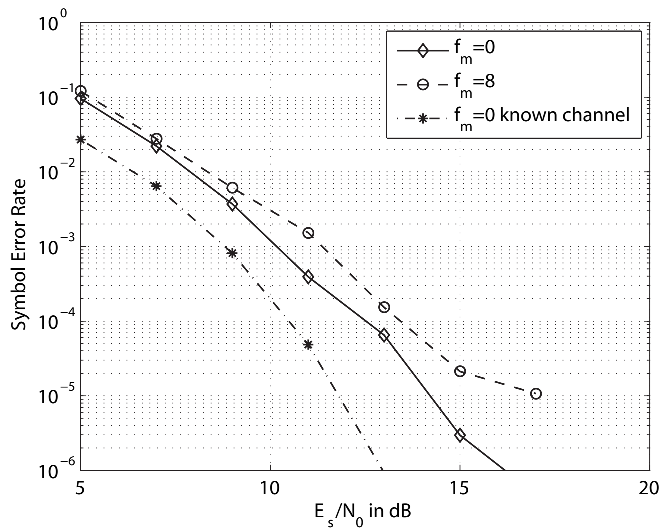

Fig. 10. Symbol error rate performance of an OFDM system with a slowly time-varying channel.

data length moderately, we are able to reduce the error rate to closely follow the ideal channel case.

D. Time-Varying Channels

We must test the proposed scheme against time-varying channels. There is a delay from sending MS data back to the BS. The round trip propagation delay is the minimum delay before FL channel estimate is immediately used at the transmitter. Because of the delay in estimating FL channels, the OFDM pre-processing will be affected by time-varying channel characteristics such as the Doppler shift.

When the channel is time varying, the channel tracking error grows with Doppler spread due to MS mobility. We test the proposed feedback scheme on a 2.4 GHz OFDM system where the BS and the MS are 1 km apart. We generate time varying taps in the 2-ray multipath model using the well known model of

$$\alpha_i(t) = \sum_{n=1}^{100} \exp\{j2\pi f_n(t)t + \theta_n\} \tag{59}$$

where $f_n(t)$ is the Doppler frequency, and θ_n is the random phase. We update the time varying channel coefficients at the OFDM packet rate. The symbol error rate performance for a pedestrian speed (1 m/s) mobile is shown in Fig. 10. In these results, we fix the RL feedback data size to $n = 100$. Bit and power loading are applied. At this moderate frame size (1 ms) and mobile speed, the resulting symbol error rate is mildly degraded, indicating that the proposed bent-pipe feedback FL channel estimation approach is suitable for slow to moderately time-varying channels.

VI. Conclusions

Generalizing the framework of a bent-pipe feedback approach to forward link channel estimation, we present a FL channel estimation scheme for wireless OFDM multicarrier systems. Estimating the FL channel directly at the transmitter, this method enables quick and direct implementation of the subcarrier bit loading and adaptive power allocation in OFDM. Detailed performance analysis of the proposed channel estimation scheme is achieved via Cramer Rao lower bound evaluation and numerical simulations.

Appendix
Knowledge Based Estimation Algorithm

Once the RTC response is obtained, a subspace algorithm similar to [12] can be applied to unravel $H(z)$ and $G(z)$ from $\mathbf{F}(z)$ under channel assumptions.

With probability one, Condition 1 holds and the polyphase components $H_i(z)$ do not share any common roots. The following relation holds from (9)

$$\mathcal{T}_m(F_{ji}) = \mathcal{T}_m(H_i)\mathcal{T}_{m+l_h}(G_j). \tag{60}$$

$\mathcal{T}_m(A)$ is the Toeplitz filtering matrix defined in (24). Define

$$\mathbf{H} = \left(\mathcal{T}_m^T(H_0) \quad \mathcal{T}_m^T(H_1) \quad \cdots \quad \mathcal{T}_m^T(H_{M-1})\right)^T, \tag{61}$$

$$\mathbf{G} = \left(\mathcal{T}_{m+l_h}(G_0) \quad \cdots \quad \mathcal{T}_{m+l_h}(G_{N-1})\right), \tag{62}$$

and

$$\mathbf{F}_i(m) = \left(\mathcal{T}_m(F_{0i}) \quad \cdots \quad \mathcal{T}_m(F_{(N-1)i})\right). \tag{63}$$

Stacking the subchannel matrices $\mathbf{F}_i$ gives

$$\mathbf{F} = \left(\mathbf{F}_0^T(m) \quad \cdots \quad \mathbf{F}_{M-1}^T(m)\right)^T. \tag{64}$$

Therefore, (6) can be re-written as

$$\mathbf{F} = \mathbf{HG} + \mathbf{N}, \tag{65}$$

where $\mathbf{N}$ is the noise. For sufficiently large m [12], $\mathbf{H}$ has full column rank, and the left null space of $\mathbf{H}$ provides $H_i(z)$ to within a scaling constant. Performing a singular value decomposition (SVD) on $\mathbf{F}$, we now have

$$\mathbf{F} = \mathbf{HG} + \mathbf{N} = (\mathbf{U}_s \quad \mathbf{U}_n)\begin{pmatrix}\mathbf{\Sigma}_s & 0\\ 0 & \mathbf{\Sigma}_n\end{pmatrix}\begin{pmatrix}\mathbf{V}_s^H\\ \mathbf{V}_n^H\end{pmatrix} \tag{66}$$

where $(\cdot)^H$ denotes the Hermitian operation. The column vectors of $\mathbf{U}_n$ span the left null space of $\mathbf{F}$ and hence that of $\mathbf{H}$. Denote $\boldsymbol{p}_i$ the i-th column vector of $\mathbf{U}_n$. Following the subspace method in [12], it can be shown that the estimation of $H(z)$ is obtained by minimizing the quadratic form

$$q(\boldsymbol{h}) = \boldsymbol{h}^H\mathbf{Q}\boldsymbol{h} \tag{67}$$

under the constraint that $\|\boldsymbol{h}\| = 1$. The forward link vector $\boldsymbol{h}$ is defined as

$$\boldsymbol{h} = (h_0(0) \ \cdots \ h_0(l_h) \ \cdots \ h_{M-1}(0) \ \cdots \ h_{M-1}(l_h))^T. \tag{68}$$

Matrix $\mathbf{Q}$ consists of columns $\boldsymbol{p}_i$, $0 \le i \le mM - l_h - m$.

Having solved $\boldsymbol{h}$ of (67) or equivalently $\boldsymbol{H}$, one way to extract the RL response $\mathbf{G}$ is to use

$$\mathbf{G} = \mathbf{H}^{\dagger}\mathbf{F}, \tag{69}$$

where $(\cdot)^{\dagger}$ denotes the (Moore-Penrose) pseudo-inverse.

When $H_i(z)$ has a common delay factor, certain columns of $\mathbf{F}$ are zero. Remove the zero columns from $\mathbf{F}$ gives $H(z)$ to within a scaling and delay factor. A similar algorithm can be derived when condition 2 holds.

REFERENCES

[1] J. van de Beek, O. Edfors, M. Sandell, S. Wilson, and P. Börjesson, "On channel estimation in OFDM systems," in *Proc. IEEE Veh. Tech. Conf.*, vol. 2, July 1995, pp. 815-819.

[2] P. Hoeher, S. Kaiser, and P. Robertson, "Two-dimensional pilot-symbolaided channel estimation by Wiener filtering," in *Proc. IEEE International Conf. on Acoustics, Speech and Signal Processing*, vol. 3, Apr. 1997, pp. 1845-1848.

[3] Y. Li, J. L. J. Cimini, and N. Sollenberger, "Robust channel estimation for OFDM systems with rapid dispersive fading channels," *IEEE Trans. Commun.*, vol. 46, pp. 902-915, July 1998.

[4] P. Chow, J. Cioffi, and J. Bingham, "A practical discrete multitone transceiver loading algorithm for data transmission over spectrally shaped channels," *IEEE Trans. Commun.*, vol. 43, no. 2/3/4, pp. 773–775, Feb./Mar./Apr. 1995.

[5] W. Yu and J. Cioffi, "On constant power water-filling," in *Proc. IEEE International Conf. on Commun.*, June 2001, pp. 1665-1669.

[6] H. Xu, S. Dasgupta, and Z. Ding, "A novel channel-identification method for wireless communication systems," *IEEE Trans. Commun.*, pp. 1767–1776, Oct. 2004.

[7] X. Dong, Z. Ding, and S. Dasgupta, "Forward link channel estimation and precoding based on decimated feedback," *IEEE Signal Process. Lett.*, 2005.

[8] P. Vaidyanathan and B. Vrcelj, "On power allocation for generalized cyclic-prefix based channel equalizers," in *Proc. IEEE International Symp. on Circuits and Systems*, vol. 1, May 2002, pp. I1-I4.

[9] P. Vaidyanathan, *Multirate Systems and Filter Banks*. Prentice Hall, 1992.

[10] G. Williamson, S. Dasgupta, and M. Fu, "Adaptive multirate, multistage filters," in *Proc. International Conference on Acoustics, Speech and Signal Processing*, 1996, pp. 1534-1537.

[11] X. Dong, Z. Ding, and S. Dasgupta, "Fractional spaced dual channel estimation based on decimated feedback," in *Proc. IEEE Wireless Commun. and Networking Conf.*, Mar. 2004, pp. 489-494.

[12] J. C. E. Moulines, P. Duhamel, and S. Mayrargue, "Subspace methods for the blind identification of multichannel FIR filters," *IEEE Trans. Signal Processing*, vol. 43, no. 2, pp. 516-525, Feb. 1995.

[13] T. Kailath, *Linear Systems*. Prentice-Hall, 1980.

[14] Z. Ding, "Multipath channel identification based on partial system information," *IEEE Trans. Signal Processing*, pp. 235-240, Jan. 1997.

[15] L. Tong and S. Perreau, "Multichannel blind identification: from subspace to maximum likelihood methods," *Proc. IEEE*, pp. 1951–1968, Oct. 1998.

[16] S. Haykin, *Adaptive Filter Theory, 3rd ed.* Prentice Hall, 1996.

[17] L. Scharf, *Statistical Signal Processing: Detection, Estimation, and Time Series Analysis*. Addison-Wesley Publishing Company, 1990.

[18] E. D. Carvalho and D. Slock, "Cramer-Rao bounds for semi-blind, blind and training sequence based channel estimation," in *Proc. First IEEE Workshop Signal Processing Advances Wireless Commun.*, pp. 129-132, 1997.

[19] E. de Carvalho and D. Slock, "Maximum-likelihood blind FIR multichannel estimation with Gaussian prior for the symbols," in *Proc. IEEE International Conference on Acoustics, Speech, and Signal Processing*, Munich, Germany, Apr. 1997, pp. 3593-3596.

[20] T. S. Rappaport, *Wireless Communications: Principles and Practice*. Prentice Hall PRT, 1996.

[21] A. Leke and J. Cioffi, "Impact of imperfect channel knowledge on the performance of multicarrier systems," in *Proc. IEEE Global Telecommun. Conf.*, vol. 2, Nov. 1998, pp. 951-955.

Xiaofei Dong received the Ph.D. degree in Electrical and Computer Engineering from the University of California, Davis in 2006. She received the M.S. degree from the University of Alberta, Edmonton, Canada in 2001, and the B.E. degree from Xi'an Jiaotong University, Xi'an, China in 1999, both in Electrical and Computer Engineering. Since 2006 she has been a senior applications engineer at Altera Corp., San Jose, CA. Her research interests are in cost effective design and implementation of digital signal processing algorithms.

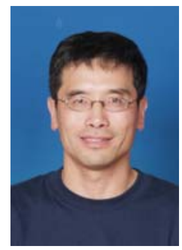

Zhi Ding is a professor at the University of California, Davis. He received his Ph.D. degree in Electrical Engineering from Cornell University in 1990. From 1990 to 2000, he was a faculty member of Auburn University and later, the University of Iowa. Prof. Ding has held visiting positions in Australian National University, Hong Kong University of Science and Technology, NASA Lewis Research Center, and USAF Wright Laboratory. He is also a guest Changjiang Chair Professor of Southeast University in Nanjing, China.

Dr. Ding is a Fellow of the IEEE and has been an active member of IEEE, serving on technical programs of several workshops and conferences. He was associate editor for the IEEE TRANSACTIONS ON SIGNAL PROCESSING from 1994-1997, and 2001-2004. He was a member of the technical committee on Statistical Signal and Array Processing and a member of the technical committee on Signal Processing for Communications (1994-2003). Dr. Ding was the Technical Program Chair of the 2006 IEEE Globecom.

Soura Dasgupta (M'87-SM'93-F'98) was born in 1959 in Calcutta, India. He received the B.E. degree in Electrical Engineering from the University of Queensland (Australia), in 1980, and the Ph.D. in Systems Engineering from the Australian National University in 1985. He is currently a Professor of Electrical and Computer Engineering at the University of Iowa, U.S.A. In 1981, he was a Junior Research Fellow in the Electronics and Communications Sciences Unit at the Indian Statistical Institute, Calcutta. He has held visiting appointments at the University of Notre Dame, University of Iowa, Universitäe Catholique de Louvain-La-Neuve, Belgium and the Australian National University. Between 1988 and 1991, and 2004 and 2007 he respectively served as an Associate Editor of the IEEE TRANSACTIONS ON AUTOMATIC CONTROL and the Associate Editor of the IEEE TRANSACTIONS ON CIRCUITS AND SYSTEMS-II. He is a corecipient of the Gullimen Cauer Award for the best paper published in the IEEE TRANSACTIONS ON CIRCUITS AND SYSTEMS in 1990 and 1991, a past Presidential Faculty Fellow, an Associate Editor for the IEEE Control Systems Society Conference Editorial Board, a subject editor for the *International Journal of Adaptive Control and Signal Processing*, and a member of the editorial board of the *EURASIP Journal of Wireless Communications*. His research interests are in controls, signal processing, and communications.